Journal of Advanced Research in Applied Sciences and Engineering Technology

Journal homepage:
https://semarakilmu.com.my/journals/index.php/applied_sciences_eng_tech/index
ISSN: 2462-1943

Narrative Review on Advances in Measurement of Electrical Properties of Materials using Free Space Method

Renukka Sivakumar[1,*], Saidatul Norlyana Azemi[2], Lee Yeng Seng[3], Kok Yeow You[3], Ping Jack Soh[5]

[1] Faculty of Electronic Engineering Technology, Universiti Malaysia Perlis, Kampus Alam UNIMAP Pauh Putra, 02600 Arau, Perlis, Malaysia
[2] Advanced Communication Engineering, Centre of Excellence (COE), Universiti Malaysia Perlis, 02600 Arau, Perlis, Malaysia
[3] Faculty of Electrical Engineering, Universiti Teknologi Malaysia, Skudai, 81310 Johor Bahru, Johor, Malaysia
[4] Centre of Wireless Communications (CWC), University of Oulu, 90570, Oulu, Finland

Keywords:

Material measurement techniques; Electrical properties; Millimetre-wave; Free space material measurement

ABSTRACT

The free-space measurement technique is a widely used method for determining the electrical characteristics of materials. The free-space measurement approach had attracted more attention due to the possibility of efficient measurements using higher millimetre-wave and terahertz frequencies. This is primarily due to its ease of use, non-destructive features, and ability to perform reflection and transmission measurements without making physical interaction with the sample. This paper discusses free space material measurement systems, beginning with the various measurement methods available for material characterization, their key concepts, post-processing in determining their properties, and advancing to their use at higher frequencies. In addition, this study discusses dielectric material characterization utilizing the free space approach, with an emphasis on their applicability to higher frequencies. This study also examined the algorithms for conversion methods and the application of lenses in free space material measurement system. Prior to the conclusion, a prospective view on the potential of this free space method was presented.

1. Introduction

Over the last two decades, there has been significant development in millimetre wave (mm- wave) and terahertz (THz) technologies, driven by their appealing properties in various applications, including automotive paint materials, metamaterial structures, radio astronomy, military, and medical fields [1-3]. Research has been conducted to study different metamaterial structures and determine their permeability [1]. Additionally, the use of dielectric properties for material identification has proven valuable in mm-wave imaging systems [2]. As a result of the increased demand for mm-wave components and systems, there is a greater need for cost-effective measurement solutions in this frequency range and beyond.

* *Corresponding author.*
E-mail address: renukkasivakumar@gmail.com

https://doi.org/10.37934/araset.56.1.266284

A crucial step in designing devices that operate at these frequencies is to determine the electrical properties of materials. These properties significantly influence the design of radio components, as their characteristics vary with frequency. Currently, most materials are typically characterized using microwave bands, highlighting the importance of addressing this need. Moreover, material characterization can be extended to assess the quality of agricultural and industrial products, as well as for biomedical applications [4,5]. Material characterization also aids in biodegradable bone screws, chitosan and rubberwood sawdust [6-8].

Various measurement techniques have been established to measure dielectric properties, specifically permittivity and permeability, at microwave frequencies. These techniques include the waveguide method, free space method, transmission line method, cavity method, and coaxial probe methods [9-14]. The free space measurement approach is particularly common among these methods due to its ability to make reflection and transmission measurements with no physical interaction with the sample [15]. The horn antennas serve as the receiver and transmitter, respectively, with the material under test (MUT) setup between them [16,17]. In order to automate, calibrate free space measurements, and calculate a material's electromagnetic properties, software was built into the system.

With the increasing portability of measurement equipment, such as vector network analysers (VNAs), and the growing significance of mm-wave/THz material spectroscopy, the free space measurement technique is expected to gain more research and commercial interest in the future. However, when applying the free space technique at higher frequencies, starting from the W-band (75 GHz) and beyond, challenges arise due to antenna beam growth, resulting in less energy being concentrated on the dielectric slab [18]. To mitigate inaccuracies during these measurements, dielectric lens was employed to focus the beam [19]. Moreover, Through-Reflect-Line calibration technique proves effective in minimizing most errors associated with the free space method [19,20].

This paper aims to reevaluate dielectric material characterization with the free space method, particularly concentrating on its extension towards higher frequencies. Initially, the paper provides an overview of the properties and types of material measurement techniques, as well as suitable material types and forms. Additionally, it explores the conversion algorithms used in dielectric material characterization [21]. In the subsequent sections, this paper delves into the various aspects of the free space measurement technique. The paper also provides the calibration methods, algorithms, and the calculations used to determine dielectric properties. The paper also explores methods to enhance measurement accuracy and emphasizes the importance of employing this technique in terahertz (THz) applications [22]. Moreover, the choice of appropriate parameter extraction algorithms holds great importance, as these elements have a substantial influence on extraction speed and accuracy across various measurement techniques.

This review distinguishes itself from other similar reviews presented in [23,24] by providing a comprehensive analysis of dielectric measurements in general, considering the frequency range and different potential methods. This review holds particular importance as it provides a comprehensive examination of the potential obstacles and concerns that arise when extending the free space method into the higher millimetre-wave frequencies (100-300 GHz), effectively addressing a critical void in current understanding.

2. Permittivity and Permeability

Electric permittivity, denoted as ε, characterizes the energy stored within an electric field and is expressed as the ratio of a material's permittivity (εr) to the permittivity of a vacuum (εo) as referenced in [25]. It also signifies a material's interaction with electric fields, often referred to as the

dielectric constant (k in Eq. (1)). The real component of permittivity, εr', quantifies the energy stored within the material, while the imaginary component, εr'', serves as the loss factor, determining the material's loss when subjected to an external electric field. In Eq. (2), magnetic permeability, denoted as μ, represents the energy stored within a magnetic field, with μo representing the permeability of free space. Figure 1 illustrates the interaction of electromagnetic fields and the relationship between permittivity and permeability, as described in [25].

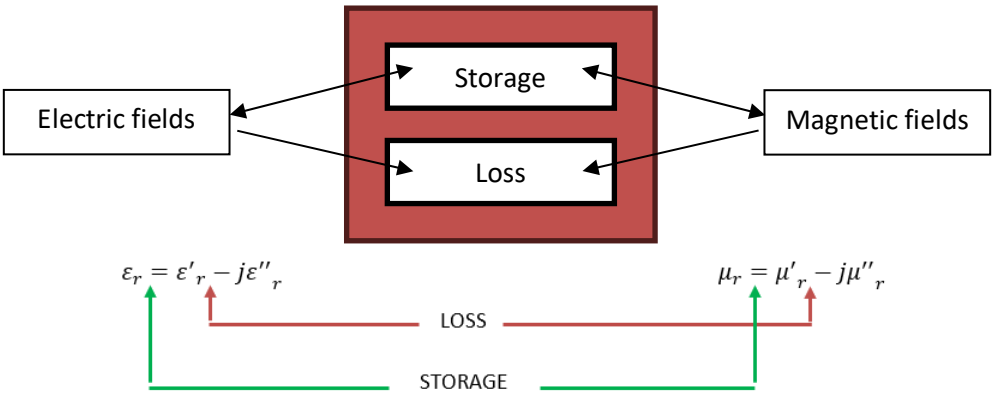

Fig. 1. The interface of electromagnetic fields and the correlation between permeability and permittivity are elucidated in reference [25]

$$\mu_r = \frac{\mu}{\mu_o} \tag{1}$$

$$\varepsilon_r = \frac{\varepsilon}{\varepsilon_o} \tag{2}$$

3. Techniques for Dielectric Properties Measurement

In this section, we will provide a concise overview of the various material property measurement techniques and evaluate their appropriateness for specific applications, as outlined in [26]. Figure 2 offers a summary of widely recognized material measurement techniques. Each of these techniques operates within distinct frequency ranges, tailored to specific frequencies, applications, and material types. Notably, the free-space measurement technique demonstrates versatility, spanning a broad frequency range from 5 GHz to 330 GHz. In contrast, the transmission line measurement technique covers the range of 50 MHz to 60 GHz, while the coaxial probe measurement capability extends from 50 MHz to 40 GHz. The resonant cavity method is typically used for materials measured between 5 GHz and 20 GHz. On the other hand, the parallel plate measurement technique is limited to frequencies up to 50 MHz. Coaxial probe and transmission line methods exhibit relatively high losses, whereas parallel plate and free space techniques show moderate losses. Among these methods, the resonant cavity method features the lowest loss.

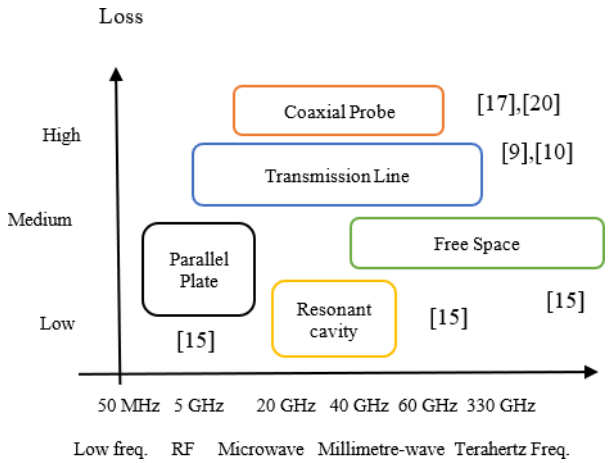

Fig. 2. Measurement ranges of various methods

Table 1 presents an overview of material measurement techniques, including their operating frequencies, types of dielectric properties measured, suitable materials for each technique, levels of losses, and measurement conversion techniques [26]. The free-space measurement technique is capable of measuring material permittivity and permeability by extracting and calculating S-parameters across a wide range of frequencies. The transmission line method shares similar capabilities but with a different frequency range. In contrast, the coaxial probe method can only extract S_{11} and consequently, retrieve ε_r. On the other hand, the resonant cavity method is unique in which it determines both the permeability and permittivity of a material. Additionally, it extracts the quality factor (Q-factor) and resonant frequency of microwave resonators from their S-parameters. Regarding losses, the coaxial probe method exhibits the highest loss, while the resonant cavity method demonstrates low loss. The free space and transmission line techniques fall into the category of medium loss.

Table 1
Comparison of Different Material Measurement Techniques [26]

Measurement techniques	Coaxial probe	Transmission line	Free space	Resonant cavity
Operating frequency	50 MHz-50 GHz	50 MHz- 60 GHz	5 GHz-330 GHz	5 GHz-20 GHz
Dielectric properties	ε_r	ε_r , μ_r	ε_r , μ_r	ε_r , μ_r
S-parameters	S_{11}	S_{11}, S_{21}	S_{11}, S_{21}	*Q*-factors
Materials	Biological specimens, liquids	Waveguide	Large solids, liquids	Solid materials, liquids, waveguides
Loss	High	Medium	Medium	Low
Conversion techniques	RFM	NRW, NIST iterative	NRW, NIST iterative	Frequency & *Q*-factors

Furthermore, both the transmission line and free space methods utilize the same conversion techniques, such as the NRW and NIST iterative methods. In contrast, the coaxial probe method employs the RFM conversion technique. The resonant cavity method stands apart from others as it uses frequency and Q-factors for the conversion technique.

3.1 Free Space Method

A free-space measurement setup comprises several components: a Vector Network Analyzer (VNA), horn antennas, a sample holder, and measurement software. In this setup, both horn antennas function as the transmitter and receiver, while the material under test (MUT) is positioned between them [21]. The measurement software plays a crucial role in automating the process of obtaining relative complex permittivity (ε_r) and relative complex permeability (μ_r) measurements through S-parameters acquired by the VNA. For instance, Keysight Technologies offers a commercial materials' measurement software that simplifies the measurement of ε_r and μ_r using a VNA, as depicted in Figure 3 [21]. This software is particularly useful for determining the dielectric properties of materials in various applications, including agriculture, biomedical, and material engineering.

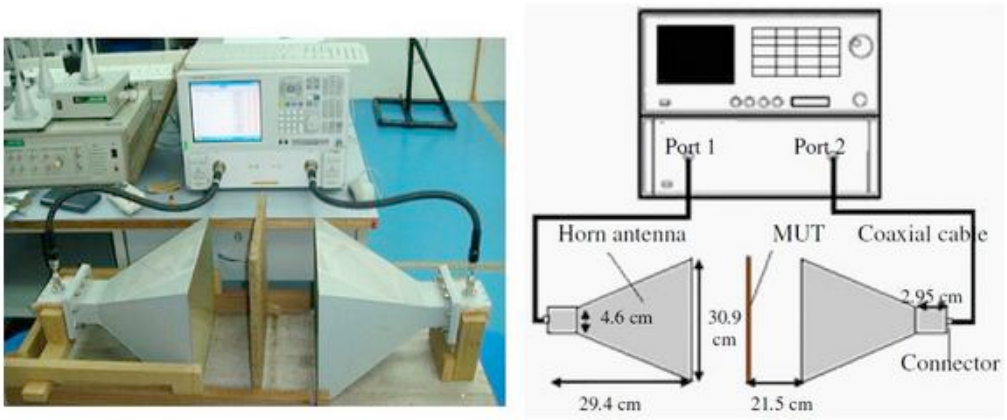

Fig. 3. Free space method [21]

3.2 Open-Ended Coaxial Probe Method

This method employs a coaxial probe with its probe aperture inserted into liquids or semi- solids to determine their permittivity, as illustrated in Figure 4 [27]. The Vector Network Analyzer (VNA) is utilized to determine the reflection coefficient (Γ), which is then converted into relative complex permittivity (ε_r). The calibration process for the coaxial probe involves short-circuit, open-circuit, and broadband and load standards, known as the open-short-load (OSL) calibration method. This technique also can be employed for measuring the dielectric properties of biological tissues [27].

In Figure 4, the schematic of the measurement setup for the open-ended coaxial probe method is presented, involving the use of the VNA to determine dielectric properties over a frequency range of 50 MHz to 50 GHz. The sample preparation for this method is straightforward, as it does not require machining of the sample. However, air gaps during the measurement process may potentially impact the accuracy of the results.

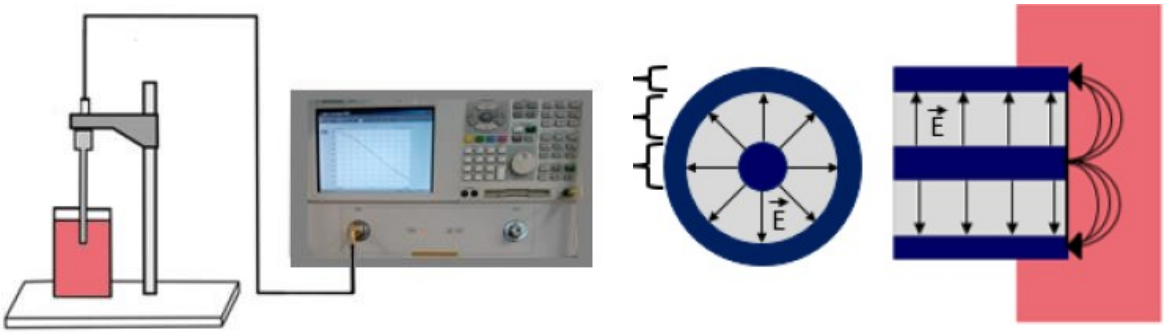

(a) (b)

Fig. 4. Open-ended coaxial probe technique: (a) a diagrammatic representation of the measurement setup, showing the Vector Network Analyzer (on the right), a cable attaching one of the VNA's ports to the coaxial probe, a probe bracket, and the liquid sample being measured; (b) top and side cross-sections of the coaxial probe, with the orientation of the electric field shown [27]

3.3 Transmission Lines

Using a Vector Network Analyzer (VNA) and a frequency range of 50 MHz to 60 GHz, measurements are made on a sample that has been placed inside a portion of the coaxial line. Before the actual measurements, the VNA undergoes calibration to ensure accuracy. Following the acquisition of the S-parameters, the dielectric characteristics is converted using specialized conversion techniques, such as the Nicholson Ross Weir (NRW) method or NIST iterative techniques. According to [18], Eq. (3) to Eq. (9) are commonly solved using either internal or external software for the NRW approach. The measurement setup is visually represented in Figure 5 [21].

One of the significant advantages of this method is its capability to determine both the permeability and permittivity of the samples. However, one of the limitations to be aware of is the potential impact of air gaps during the measurement process, which may influence the accuracy of the results.

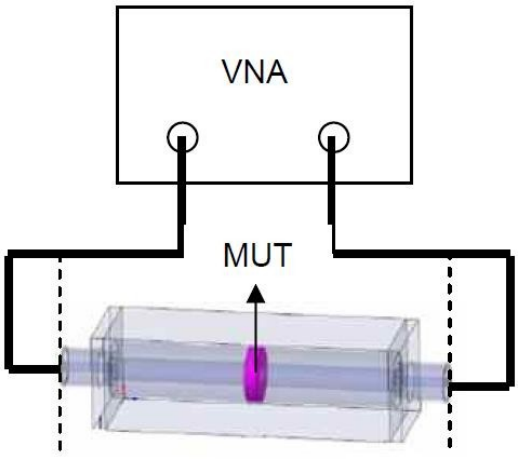

Fig. 5. Transmission-Reflection method [21]

3.4 Resonant Cavity Technique

By using cavities that resonate at particular frequencies, the resonant cavity method is used to analyse the material properties of liquids, waveguides, and rod-shaped solid materials. Although it is

limited to a single, fixed frequency, it offers improved measurement accuracy. When material samples are inserted into the cavity, the way they interact with the electromagnetic field causes a shift in the measured resonance and Q-factor, leading to the determination of the sample's properties. For a visual representation of the resonant cavity method, refer to Figure 6 [21].

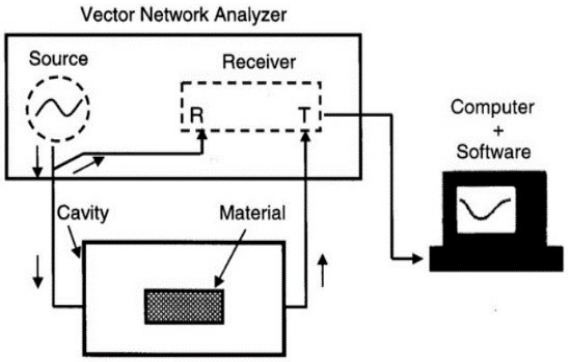

Fig. 6. Resonant method [21]

4. Algorithms for calculation of material properties

In free-space measurement systems, various conversion methods are employed to calculate the final dielectric properties [21]. The selection of a suitable conversion method depends significantly on the required speed and accuracy in determining these properties [21]. Table 2 provides an overview of the algorithms and appropriate conversion methods used for different types of material measurements [21]. The three main algorithms are:

i. NRW [21]
ii. NIST iterative [21]
iii. New non-iterative [21]

Table 2
Algorithms and Calculations in measurement methods [21]

Materials/ Length/ Magnetic Properties	Measurement methods	Conversion methods	Speed	Accuracy
Lossy solids, short, non-	TR	NRW	Fast	Medium
Biological specimen, Liquids	Coaxial probe	RFM	Fast	Good
High temperature	Free-	NRW	Fast	Good
Solids, large/flat, space non-magnetic				
Low loss solids,	Resonant	Frequency& *Q*-factors	Slow	Good

4.1 Nicolson-Ross-Weir (NRW) Technique

The Nicolson Ross Weir (NRW) approach, which is quick, non-iterative, and allows for wide frequency band characterization, could be used to determine the permeability and permittivity [28]. The explicit calculation of both r and r from S-parameters can be done using this method, which is recommended [29]. The NRW algorithm's flow is shown in Figure 7, according to [21]. The permeability and permittivity of the test material are predicted using the measured broadband S-parameters (reflection and transmission coefficients) from a VNA. One of the methods to determine *n* is through the analysis of group delay. The phase ambiguity could be solved by comparing the

measured group delay, $\tau meas$ shown in Eq. (4), and the calculated group delay, τcal in Eq. (3), to find the correct value of n. Eq. (5) can be used when $n= k$.

$$\tau_{cal} = \frac{1}{c^2} \frac{f\varepsilon_r\mu_r + f^2 \frac{1}{2} \frac{d(\varepsilon_r\mu_r)}{df}}{\sqrt{\frac{\varepsilon_r\mu_r f^2}{c^2} - \frac{1}{\lambda c^2}}} L \tag{3}$$

$$\tau_{meas} = -\frac{1}{2\Pi \frac{d\Phi}{df}} \tag{4}$$

$$\tau_{cal} - \tau_{meas} = 0 \tag{5}$$

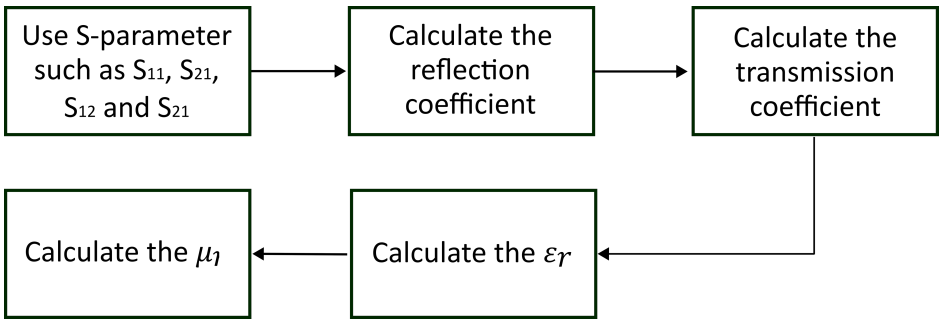

Fig. 7. Flow of NRW method [21]

The NRW approach was used as an example to determine the physical characteristics of concrete using NRW [30]. Dielectric constant measurements were used to assess the electrical properties of concretes with various water/cement (w/c) ratios, and the relationship between their electrical and mechanical properties was investigated. The compressive strength, splitting tensile, abrasion resistance, water absorption, and high-pressure water penetration qualities of the concrete are all influenced by the w/c ratio. By choosing these w/c ratios, the compressive strengths of the samples controlled, allowing for control of the other mechanical and transport factors. Increasing the water content of concrete results in a weaker link between the cement paste and the aggregates, wider capillary holes, and a more heterogeneous mixture due to segregation as compared to concretes with a lower w/c ratio. The measurement setup for this work is shown in Figure 8 below [30].

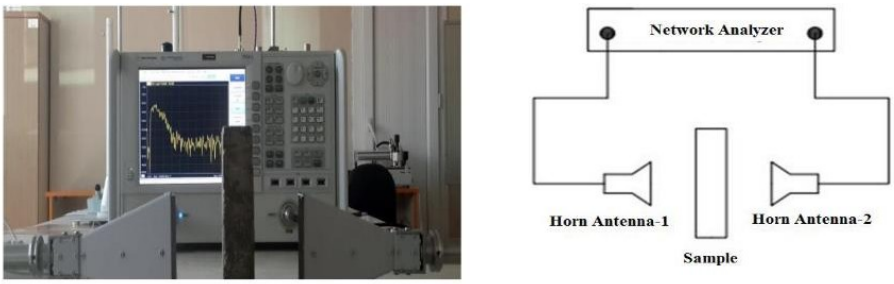

Fig. 8. Measurement setup [30]

The use of focusing horn or lens antennas and appropriate calibration techniques, such as those in [31], can be used to address the inaccuracies in measurements of dielectric materials. As shown in Figure 9 [31], several studies on the frequency-by-frequency approach have been proposed. These studies include NRW (Transmission and Reflection Algorithm), TO (Transmission-Only Algorithm), and RO (Reflection-Only Algorithm). The use of focusing horn or lens antennas and appropriate

calibration techniques, such as those in [31], can be used to address the inaccuracies in measurements of dielectric materials. As shown in Figure 9 [31], several studies on the frequency-by-frequency approach have been proposed. These studies include NRW (Transmission and Reflection Algorithm), TO (Transmission-Only Algorithm), and RO (Reflection-Only Algorithm). The parameter is calculated using the function's root, F. When S21 is not available, the scattering model is employed in Eq. (6) FR of the slab. Using a permeability of r = 1, the RO (Reflection-Only) algorithm, FRO, is utilized to solve Eq. (1). On the other hand, in order to solve Eq. (9)—an equation for the transmission coefficient, FT for the slab scattering model—using the TO (Transmission- Only) technique, FTO, r =1 is also presupposed.

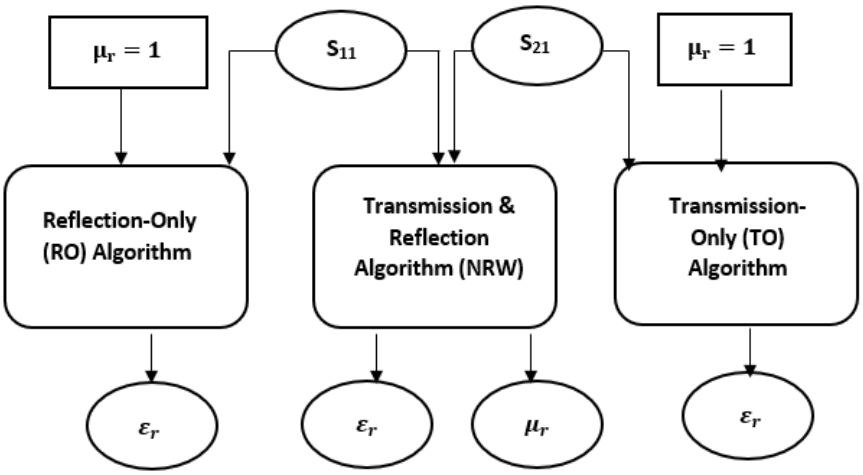

Fig. 9. Calculation strategies for free space measurement systems are represented [31]

$$F_R(\varepsilon_r, \mu_r, \sigma) = \frac{j(y^2-1)\tau}{2y+j(y^2+1)\tau} \quad (6)$$

$$F_{RO} = S_{11} + \frac{(\varepsilon_r-1)\tan(v)}{2\sqrt{\varepsilon_r}+j(\varepsilon_r+1)\tan(v)} = 0 \quad (7)$$

$$F_T(\varepsilon_r, \mu_r, \sigma) = \frac{2y}{\cos\left(\frac{wxd}{c}\right)[2y+j(y^2+1)\tau]} \quad (8)$$

$$F_{TO} = S_{21}\left[\varepsilon_r \cos(v) + j\sqrt{\frac{\varepsilon_r}{4}}(1+\varepsilon_r)\sin(v)\right] - \varepsilon_r = 0 \quad (9)$$

One of the issues that the NRW method suffers from is the phase ambiguity which is caused by the branching problem of the algorithm. This occurs when $-\infty \leq m \leq \infty$, where the results obtained are accurate up to the value of m = 0. Beyond that, phase ambiguities will increase especially for thicker materials. To overcome this, the NRW method has been modified for improved measurement accuracy, especially for nanostructured materials with better accuracy [32]. The intrinsic impedance of the slab, η is extracted directly from the scattering coefficients [32]. Parameter k is the phase constant, *d* is the thickness of the slab, and *n* is the refractive index (with η′ and η′′ its real and imaginary refractive index). Intrinsic impedance which has sign ambiguity in Eq. (10) can be solved by allowing Re (n)≥0. In Eq. (11), the branching value, *m* is unknown. From Eq. (12), η′′ can be determined ambiguously with the use of value m, which solves the ambiguity issue in NRW method [32].

$$\eta = \pm\sqrt{\frac{(1+S_{11})^2-S_{21}{}^2}{(1-S_{11})^2-S_{21}{}^2}} = \eta' \pm j\eta'' \quad (10)$$

$$\eta' = \frac{j\,ln(t)-2\pi m}{k_o d} \quad (11)$$

$$\eta'' = \frac{-Im\,g(ln(t))-2\pi m}{k_o d} \quad (12)$$

In addition, [33] addressed the solution for the branching issue in the NRW method and proposed a method of permeability and permittivity extraction applicable for any material thicknesses as shown in Figure 10.

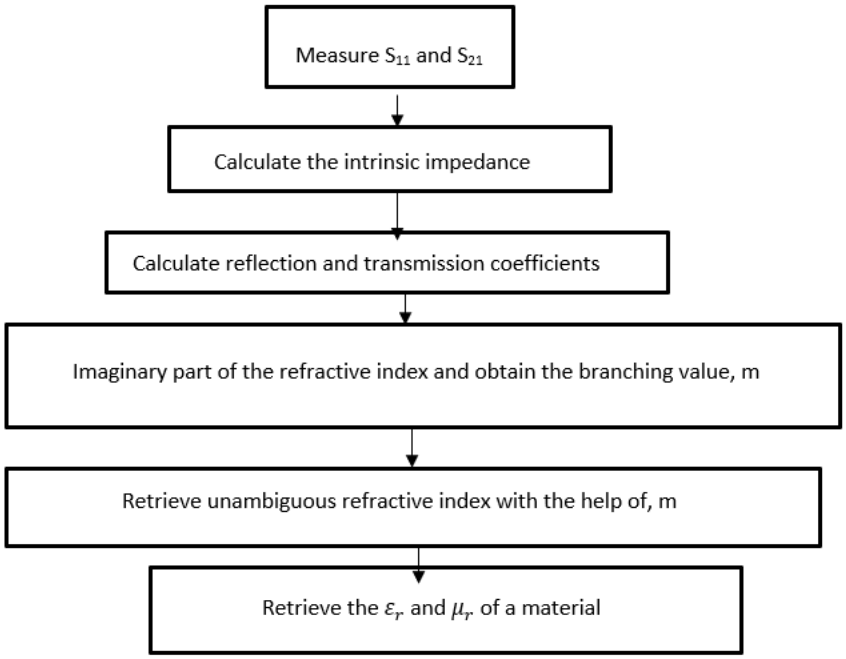

Fig. 10. Flowchart of unambiguous retrieval of material properties [33]

4.2 NIST Iterative Method

The NIST method is an alternative conversion technique capable of extracting permittivity solely from S-parameters. It proves effective for characterizing low-loss materials and long samples, as indicated in [21]. Additionally, this method yields smooth permittivity results with no divergence. However, it is essential to note that one of the limitations of the NIST method is its inability to determine permeability measurements. When compared with the NRW method, the NRW method is better as both the permeability and permittivity of materials could be determined by setting the μr = 1. Figure 11 shows the flowchart of the NIST iterative method, which starts with determining the Jacobian matrix, *J* using Newton-Raphson algorithm, followed by the calculation of permittivity, $F(\varepsilon r)$ [21]. This process is performed using Eq. (13) to Eq. (20), with its transmission coefficient denoted as *T*. Then the algorithm's convergence is checked. If the algorithm does not converge, the process continues with the finding of the inverse Jacobian matrix, J^{-1} through Eq. (18). Then the inverse Jacobian matrix is multiplied with the permittivity to obtain next estimated εr, which is denoted by Eq. (19). On the other hand, the process ends with Eq. (20) when the algorithm converges.

The propagation constant, γ of material can be expressed as:

$$\gamma = j\sqrt{\frac{\omega^2 \mu_r \varepsilon_r}{c^2} - \left(\frac{2\pi}{\lambda_c}\right)^2} \tag{13}$$

where *c* is the speed of light in free space that can be defined as:

$$c = \frac{1}{\sqrt{\varepsilon_o \mu_o}} \tag{14}$$

By substituting Eq. (20) into Eq. (19), an equation with μ_r =1 obtained as:

$$\gamma = j\sqrt{\mu_o \mu_r \varepsilon_o \varepsilon_r \omega^2 - \left(\frac{2\pi}{\lambda_c}\right)^2} \tag{15}$$

The reflection coefficient, Γ is then expressed as,

$$\Gamma = \frac{\frac{\gamma_o}{\mu_o} - \frac{\gamma}{\mu}}{\frac{\gamma_o}{\mu_o} + \frac{\gamma}{\mu}} = \frac{\gamma_o - \gamma}{\gamma_o - \gamma} \tag{16}$$

The permittivity then indicated as:

$$F(\varepsilon_r) = \frac{S_{21} + S_{12}}{2(1 - T^2\Gamma^2)} - T(1 - \Gamma^2)e^{-j\gamma_o(L_{air} - L)} \tag{17}$$

When $F(\varepsilon_r)$ =0, the algorithm is considered convergent. To determine the root, by the Newton method, the Jacobian matrix is then concluded as follows:

$$J = \begin{matrix} \frac{f_1(\varepsilon' + h, \varepsilon'') - f_1(\varepsilon' - h, \varepsilon'')}{2h} & \frac{f_2(\varepsilon', \varepsilon'' + h) - f_2(\varepsilon', \varepsilon'' - h)}{2h} \\ \frac{f_2(\varepsilon' + h, \varepsilon'') - f_2(\varepsilon' - h, \varepsilon'')}{2h} & \frac{f_2(\varepsilon', \varepsilon'' + h) - f_2(\varepsilon', \varepsilon'' - h)}{2h} \end{matrix} \tag{18}$$

By obtaining the inverse of the Jacobian matrix, small changes in the permittivity function are expressed as:

$$\Delta\varepsilon_r = J^{-1}\varepsilon_r \tag{19}$$

The algorithm can be terminated once the $F(\varepsilon_r)$ is adequately close to zero as follows,

$$\varepsilon_{r(new)} = \varepsilon_r + \Delta\varepsilon_r \tag{20}$$

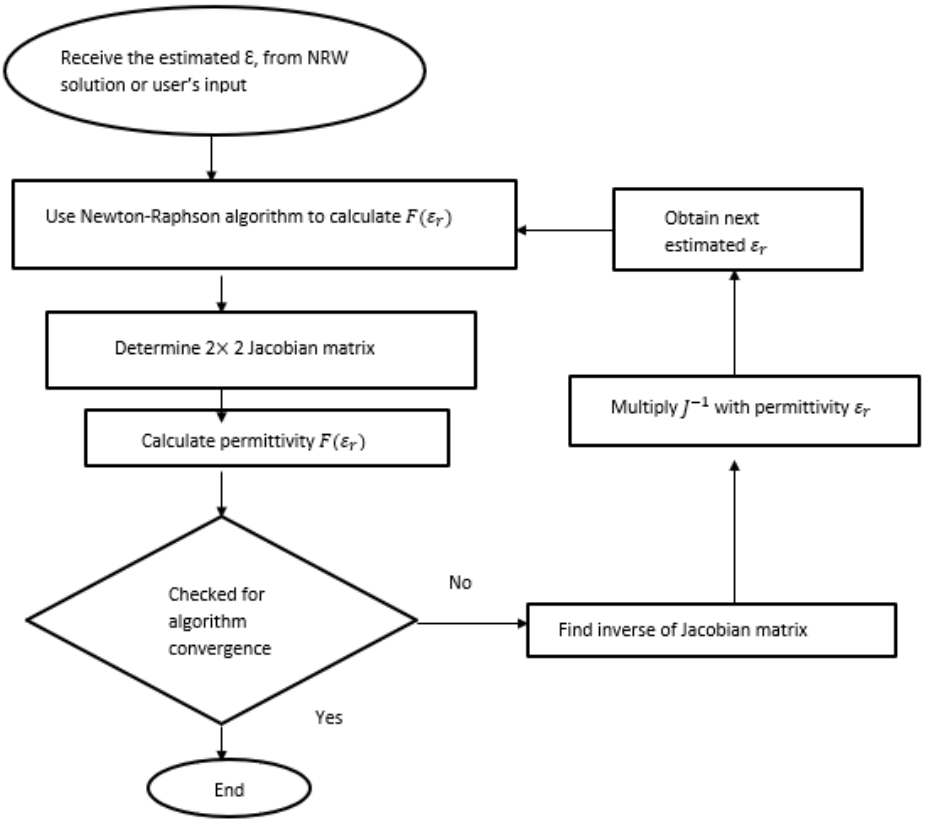

Fig. 11. Flowchart of NIST iterative method algorithm [21]

4.3 New Non-Iterative Method

The new non-iterative is quite similar to the NRW method, with the special case that it determines the effective electromagnetic parameters, which are effective permeability, μ_{eff} and effective permittivity, ε_{eff} as in Eq. (21) and Eq. (22) as in [21]. This method uses the same equations as the NRW method to compute the reflection coefficient, Γ and transmission coefficient, *T*. Then, the permeability and permittivity could be determined through Eq. (23) and Eq. (24). For the new non-iterative method, one of the advantages is that there are no divergences seen in the sample at frequencies corresponding to integer multiples of one-half wavelength when compared to both the NRW and NIST iterative approaches in [21]. One limitation of this method is that it only provides permittivity measurement. In contrast, when comparing it with the NRW method, the NRW method can determine both the permeability and permittivity, making it a more comprehensive option rather than solely providing the permittivity measurements.

The effective permeability can be expressed as

$$F(\varepsilon_r) = \frac{S_{21}+S_{12}}{2(1-T^2\Gamma^2)} - T(1-\Gamma^2)e^{-j\gamma_0(L_{air}-L)} \tag{21}$$

The effective permittivity can be defined as,

$$\varepsilon_{efff} = \frac{\lambda_{og}}{\wedge}\left(\frac{1-\Gamma}{1+\Gamma}\right) \tag{22}$$

The permeability then indicated as,

$$\mu_r = \mu_{efff} = \frac{1}{\Lambda}\left(\frac{1+\Gamma}{1-\Gamma}\right)\frac{1}{\sqrt{\frac{1}{\lambda_0{}^2}-\frac{1}{\lambda_c{}^2}}} \tag{23}$$

The permittivity then expressed as,

$$\varepsilon_r = \left(1-\frac{\lambda_o^2}{\lambda_c^2}\right)\varepsilon_{eff} + \left(\frac{\lambda_o}{\lambda_c}\right)^2\left(\frac{1}{\mu_{eff}}\right) \tag{24}$$

The NRW algorithm is commonly used despite having some drawbacks. However, many researchers have utilized the NRW algorithm and made modifications to enhance measurement accuracy [32,34]. Additionally, to address the limitations of the NRW method, one researcher proposed a new method of permeability and permittivity extraction that is applicable for any material thickness [35].

5. Extending Measurements to the Upper Millimetre-Wave Range

Two methods have been mainly proposed to extend material measurements towards the upper millimetre-wave (mmW) range:

i. the time-domain spectroscopy (TDS) method
ii. the free- space method [35].

The TDS method uses pulse waves that move through the MUT when measured in the time domain, whereas the free space method uses radio waves (*S*-parameters). In this work, the suitability of measured complex relative permittivity in the THz band was determined by comparing the complex relative permittivity obtained using a VNA with that obtained using TDS [35]. Although aligning the transmitting and receiving antennas is simple with the free- space approach, the measuring frequency is limited by the size of a waveguide. Moreover, despite the wide TDS measurement frequency range, the accuracy of the measurement is lower because the signal-to-noise ratio deteriorates at low frequencies. The positioning of the receiving and transmitting antennas was carefully adjusted to receive the maximum level. TDS alignment is more challenging than free-space alignment using a VNA. TDS method can be used for high frequencies, in which changes to the frequency domain are done through the Fourier transform. The frequency range of the measurement and the measurement precision must both be taken into consideration when choosing a measurement method. The measured complex relative permittivity by TDS and VNA were found to be within the error bar.

For the free space method, a systematic study on the measurement of dielectric properties of photopolymer from 220 GHz-320 GHz was performed in [36]. Table 3 shows the dielectric lens antenna parameters reported in this review, whereas Table 4 presents the dimensions of the designed and fabricated dielectric lens antenna [36].

Table 3
Dielectric Lens Antenna Parameters [36]

Parameter	Description	Optimum value (mm)
R	Lens radius	3.00
L	Extension Length	3.00
Fw	Fixture width	3.00
FD	Fixture diameter	1.70
FL	Fixture length	6.40
FT	Fixture thickness	2.00
a	Matching length	0.86
b	Matching width	0.43
m	Matching depth	0.20

A comparison of complex relative permittivity values was carried out using both methods for materials such as PPE, PTFE, epoxy composites, and cyclo olefin polymers in a study by [37] spanning the frequency range of 220 to 330 GHz. It's worth noting that for the TDS method, the signal-to-noise ratio deteriorates in the lower frequency bands below 300 GHz during measurements, primarily because measurement precision decreases at these broadband frequencies.

Table 4
The dimensions of dielectric lens antenna between design values and fabrication values [36]

Parameters	Design values (mm)	Actual values (mm)
R	3.00	2.96
L	3.00	2.98
FW	3.00	3.00
FP	1.70	1.72
FL	6.40	6.39
FT	2.00	1.98
a	0.86	0.87
b	0.43	0.44
m	0.20	0.22

When it comes to aligning the Vector Network Analyzer (VNA) during free-space calibration, it's generally found to be more straightforward compared to the TDS method, especially when dealing with materials of varying thicknesses, as indicated in Table 5 [37]. This table also presents the minimum and maximum thickness values for the Materials Under Test (MUTs) used in the TDS method. Variations in MUT thickness introduce dispersion and can have a significant impact on the accuracy of the complex relative permittivity measurements. This underscores the importance of precise alignment of the VNA and attention to the thickness of the MUTs when characterizing these materials.

Table 5
Material thickness of different materials And Minimum and Maximum thickness value [37]

Material No.	Material	Thickness [mm] Used for: VNA/TDS
A	PPE based resin, $TLC593$	0.483 / 0.486
B	PPE based resin, $TLC598$	0.508 / 0.506
C	PTFE/Epoxy composite, $ML620$	0.488 / 0.479
D	Glass/Epoxy composite, $R1551$	0.466 / 0.476
E	Glass/Epoxy composite,$R1661$	0.486 / 0.487
F	$Cyclo$ olefin polymer, $Zeonex$	2.025 /2.005
Material	Used for free space VNA	Used for TDS
A	0.479mm / 0.488mm	0.484mm / 0.489mm
B	0.504mm / 0.512mm	0.505mm / 0.509mm
C	0.482mm / 0.495mm	0.475mm / 0.481mm
D	0.445mm / 0.480mm	0.471mm / 0.478mm
E	0.468 mm/ 0.495mm	0.471mm / 0.498mm
F	2.001 mm/ 2.046mm	1.998mm / 2.012mm

In [38], a non-iterative extraction technique was introduced for measuring the complex permittivity of materials using the reflection-transmission based free-space method in the frequency range of 220 to 325 GHz. Notably, this method is not limited solely to cases where the measured S21 falls below the measurement instrument's threshold level; it can also be effectively employed to determine the complex permittivity of lossy materials when S_{21} exceeds the threshold.

The suggested non-iterative extraction method, designed for the reflection-transmission based free-space approach at terahertz frequencies, demonstrates its efficacy in reducing the characterization resonance [38]. For a comprehensive overview of the permittivity values of Materials Under Test (MUTs) such as Teflon, PTFE, Rogers 4350B, and air across different frequencies, please refer to Table 6 [38].

Table 6
Comparison of Teflon, PTFE, Rogers 4350B and Air Permittivity Values Based on Literature Studies According to the Frequencies [38]

MUT	Frequency (GHz)	ε_r'
Teflon	110 GHz	2.04
	850 GHz	2.042
	300 GHz	2.0535
	300 GHz	2.0442
PTFE	450 GHz	1.99
	35 GHz	1.952
	300 GHz	1.9523
Rogers 4350B	30 GHz	3.71
	300 GHz	3.7692
Air	300 GHz	1.0021

In [39], an investigation into the dielectric properties of low-loss dielectric materials was conducted within the frequency range of 220 to 325 GHz. This measurement was carried out using a bidirectional scattering measurement system, which includes components such as the sample, transmitter, receiver, receiver rotators, and Vector Network Analyzer (VNA), as illustrated in Figure

12 [39]. The transmitters and receivers are equipped with frequency up/down converters and antennas to facilitate the measurements.

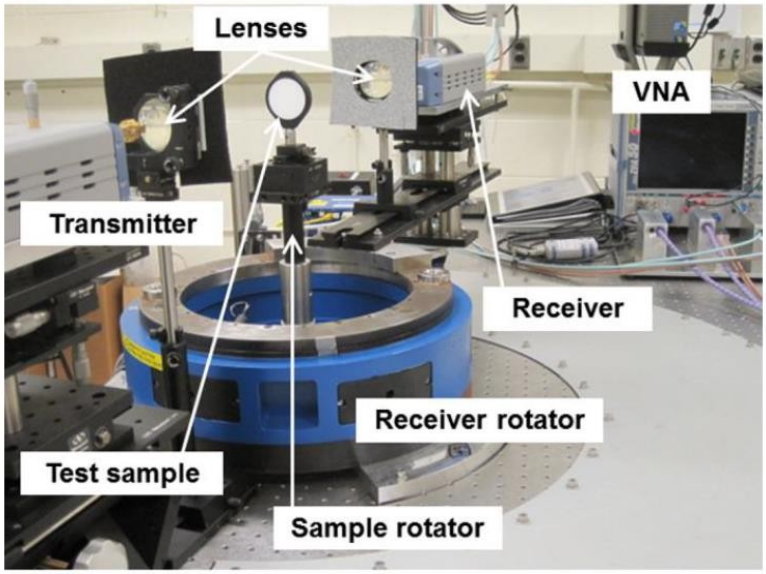

Fig. 12. Bidirectional Scattering Measurement System [39]

Various material samples were included in the measurements, as outlined in Table 7. These samples encompass two-cross-linked polystyrene, PTFE, and polymethyl pentene, allowing for a comprehensive assessment of their dielectric properties within the specified frequency range [39]. The minimum uncertainty of permittivity values occurs when θ=0, for the samples tested [39]. It has been demonstrated that as θ increases, so do the uncertainties in permittivity values. Sample thickness is important as the sample thickness causes the nominal errors in this study. According to predictions, it is typically difficult to determine the sample thickness precisely enough to obtain the permittivity using the standard free-space measuring method at very high frequencies [39].

Table 7
Sample Thickness of Different Materials [39]

Incident angle, θ (Deg.)	Sample Thickness (mm)			
	XLPS sample 1	XLPS sample 2	PTFE sample	PMP sample
0	8.90	9.94	10.71	9.93
10	8.79	9.91	10.42	10.25
20	9.03	10.05	10.03	10.11
30	8.75	9.81	10.03	10.22

In summary, measuring the complex permittivity of materials in the upper millimetre-wave (mmW) range primarily involves two main methods: the free space method based on the transmission theorem and the time-domain spectroscopy (TDS) method [37,40]. Additionally, non-iterative extraction techniques have been adopted to reduce the resonance requirements for free space measurements. Furthermore, dielectric characterization of low-loss materials in the upper mmW range can be accomplished by utilizing a bidirectional scattering measurement system. When selecting a suitable material measurement technique in this frequency band, it is crucial to consider factors such as the target frequency range, appropriate extraction techniques, and the required measurement accuracy. A high cardinality and signal power can be supported by an OCDMA system

using the new ZCC coding [41]. Optical vortex also been used in the OCDMA system to increase optical communication's capacity and security [42].

6.Conclusions

This paper provides a comprehensive review of various methods used for high-frequency electrical characterization of material properties. Various measurement methods were discussed. The choice of suitable methods depends on factors such as the material type and thickness, the parameter of interest, the frequency range, and the required accuracy. This review places particular emphasis on the measurement of a material's electrical properties, specifically its complex permittivity, employing the free space measurement method. The free space method is selected for this focus due to its versatility in characterizing different material types and thicknesses. Moreover, its potential for characterizing materials at higher millimetre-wave (mmW) frequencies is another reason for this choice. As this research area progresses, future developments in the free space measurement technique can be pursued by exploring improved calibration standards, conversion algorithms, and measurement techniques to enhance measurement accuracy.

Acknowledgement

This research was supported by the Malaysian Technical Universities' Network (MTUN) Matching Research Grant, which was awarded by the Ministry of Higher Education of Malaysia (MOHE) under Project No. UniMAP/PPPI/GRN IRPA/MTUN/9002-00101/9028-00016.

References

[1] Kumar, Amitesh, Arijit Majumder, Shantanu Das, and Subal Kar. "A Comparative Study of Different Negative Permeability Metamaterial Structures at X band: Useful for Microwave Applications." In *2018 IEEE MTT-S International Microwave and RF Conference (IMaRC)*, pp. 1-4. IEEE, 2018. https://doi.org/10.1109/IMaRC.2018.8877326

[2] Wang, Ziye, Yang Yu, Lingbo Qiao, and Ziran Zhao. "Material Identification Using Dielectric Properties with Millimeter-wave Imaging System." In *2020 Cross Strait Radio Science & Wireless Technology Conference (CSRSWTC)*, pp. 1-3. IEEE, 2020. https://doi.org/10.1109/CSRSWTC50769.2020.9372690

[3] Zou, Qiao, Rui Zhao, Jie Wu, Yahai Wang, Ziqi Jiang, and Jinbang Wang. "Broadband Millimeter Wave Dielectric Properties Measurement of Low Loss Materials." In *2021 IEEE 15th International Conference on Electronic Measurement & Instruments (ICEMI)*, pp. 498-501. IEEE, 2021. https://doi.org/10.1109/ICEMI52946.2021.9679600

[4] Lim, Sungmook, Choul-Young Kim, and Songcheol Hong. "Simultaneous measurement of thickness and permittivity by means of the resonant frequency fitting of a microstrip line ring resonator." *IEEE Microwave and Wireless Components Letters* 28, no. 6 (2018): 539-541. https://doi.org/10.1109/LMWC.2018.2833202

[5] Ab Jabal, Siti Nurbazilah, Yew Been Seok, and Wee Fwen Hoon. "Carbon composition, surface porosities and dielectric properties of coconut shell powder and coconut shell activated carbon composites." *ARPN J. Eng. Appl. Sci* 11, no. 6 (2016): 3832-3837.

[6] Ismail, Rifky, Deni Fajar Fitriyana, Athanasius Priharyoto Bayuseno, Rafi Munanda, Rilo Chandra Muhamadin, Fariz Wisda Nugraha, Andri Setiyawan *et al.,* "Design, manufacturing and characterization of biodegradable bone screw from PLA prepared by Fused Deposition Modelling (FDM) 3D printing technique." *Journal of Advanced Research in Fluid Mechanics and Thermal Sciences* 103, no. 2 (2023): 205-215. https://doi.org/10.37934/arfmts.103.2.205215

[7] Ismail, Rifky, Deni Fajar Fitriyana, Athanasius Priharyoto Bayuseno, Putut Yoga Pradiptya, Rilo Chandra Muhamadin, Fariz Wisda Nugraha, Andri Setiyawan *et al.,* "Investigating the Effect of Deacetylation Temperature on the Characterization of Chitosan from Crab Shells as a Candidate for Organic Nanofluids." *Journal of Advanced Research in Fluid Mechanics and Thermal Sciences* 103, no. 2 (2023): 55-67. https://doi.org/10.37934/arfmts.103.2.5567

[8] Phainuphong, Supawet, Juntakan Taweekun, Kittinan Maliwan, Thanansak Theppaya, Md Sumon Reza, and Abul Kalam Azad. "Synthesis and Characterization of Activated Carbon Derived from Rubberwood Sawdust via Carbonization and Chemical Activation as Electrode Material for Supercapacitor." *Journal of Advanced Research in Fluid Mechanics and Thermal Sciences* 94, no. 2 (2022): 61-76. https://doi.org/10.37934/arfmts.94.2.6176

[9] Wang, Yi, Xiaobang Shang, Nick M. Ridler, Tongde Huang, and Wen Wu. "Characterization of dielectric materials at WR-15 band (50–75 GHz) using VNA-based technique." *IEEE Transactions on Instrumentation and Measurement* 69, no. 7 (2019): 4930-4939. https://doi.org/10.1109/TIM.2019.2954010
[10] Ozturk, Turgut, and Muhammet Tahir Güneşer. "Measurement methods and extraction techniques to obtain the dielectric properties of materials." *Electrical and Electronic Properties of Materials* 6 (2018): 83-108. https://doi.org/10.5772/intechopen.80276
[11] Note, Application. "Basics of measuring the dielectric properties of materials." *Agilent Technologies* (2006): 1e31.
[12] Brinker, Katelyn, Matthew Dvorsky, Mohammad Tayeb Al Qaseer, and Reza Zoughi. "Review of advances in microwave and millimetre-wave NDT&E: Principles and applications." *Philosophical Transactions of the Royal Society A* 378, no. 2182 (2020): 20190585. https://doi.org/10.1098/rsta.2019.0585
[13] Krupka, Jerzy. "Microwave measurements of electromagnetic properties of materials." *Materials* 14, no. 17 (2021): 5097. https://doi.org/10.3390/ma14175097
[14] Sato, Yasumoto, Natsuki Ogura, Yuhei Yamaguchi, and Yang Ju. "Development of a sensor for dielectric constant measurements utilizing time-domain measurement with a vector network analyzer." *Measurement* 169 (2021): 108530. https://doi.org/10.1016/j.measurement.2020.108530
[15] Akhter, Zubair, and Mohammad Jaleel Akhtar. "Free-space time domain position insensitive technique for simultaneous measurement of complex permittivity and thickness of lossy dielectric samples." *IEEE Transactions on Instrumentation and Measurement* 65, no. 10 (2016): 2394-2405. https://doi.org/10.1109/TIM.2016.2581398
[16] Ozturk, Turgut, Osamu Morikawa, İlhami Ünal, and İhsan Uluer. "Comparison of free space measurement using a vector network analyzer and low-cost-type THz-TDS measurement methods between 75 and 325 GHz." *Journal of Infrared, Millimeter, and Terahertz Waves* 38 (2017): 1241-1251. https://doi.org/10.1007/s10762-017-0410-1
[17] Semenenko, V. N., V. A. Chistyaev, A. A. Politiko, and K. M. Baskov. "Test stand for measuring the free-space electromagnetic parameters of materials over an ultrawide range of microwave frequencies." *Measurement Techniques* 62 (2019): 161-166. https://doi.org/10.1007/s11018-019-01601-5
[18] Alqahtani, Ali H., Yosef T. Aladadi, and Mohammed T. Alresheedi. "Dielectric Slabs-Based Lens for Millimeter-Wave Beamforming." *Applied Sciences* 12, no. 2 (2022): 638. https://doi.org/10.3390/app12020638
[19] Vohra, Nagma, and Magda El-Shenawee. "K-and W-band free-space characterizations of highly conductive radar absorbing materials." *IEEE Transactions on Instrumentation and Measurement* 70 (2020): 1-10. https://doi.org/10.1109/TIM.2020.3041821
[20] Zhang, Na, Junjie Cheng, Pengwei Gong, and Hongmei Ma. "A broadband free-space dielectric measurement system." In *2015 IEEE MTT-S International Microwave Workshop Series on Advanced Materials and Processes for RF and THz Applications (IMWS-AMP)*, pp. 1-3. IEEE, 2015. https://doi.org/10.1109/IMWS-AMP.2015.7324930
[21] Yaw, K. C. "Measurement of dielectric material properties application note products." *Application Note Rhode and Schwarz* 36 (2012).
[22] Sivarajan, Vysakh. "Time-domain thru-reflect-line (TRL) calibration error assessment and its mitigation and modeling of multilayer printed circuit boards (PCB) with complex area fills." (2010).
[23] Seng, Sim Man, Kok Yeow You, Fahmiruddin Esa, and Mohd Zul Hilmi Mayzan. "Dielectric and Magnetic Properties of Epoxy with Dispersed Iron Phosphate Glass Particles by Microwave Measurement." *Journal of Microwaves, Optoelectronics and Electromagnetic Applications* 19 (2020): 165-176. https://doi.org/10.1590/2179-10742020v19i2824
[24] The Evolution of Dielectric Properties Measurement Techniques for Agricultural Products." (2021).
[25] Ozerov, Ruslan P., and Anatoli A. Vorobyev. *Physics for chemists*. Elsevier, 2007.
[26] Kang, Jin-Seob, and Jeong-Hwan Kim. "GSS (Gated-Short-Short) Calibration for Free-space Material Measurements in millimeter-Wave Frequency Band." In *2019 Antenna Measurement Techniques Association Symposium (AMTA)*, pp. 1-3. IEEE, 2019. https://doi.org/10.23919/AMTAP.2019.8906376
[27] La Gioia, Alessandra, Emily Porter, Ilja Merunka, Atif Shahzad, Saqib Salahuddin, Marggie Jones, and Martin O'Halloran. "Open-ended coaxial probe technique for dielectric measurement of biological tissues: Challenges and common practices." *Diagnostics* 8, no. 2 (2018): 40. https://doi.org/10.3390/diagnostics8020040
[28] Wang, J. Y., J. Tao, L. Severac, D. Mesguich, and Ch Laurent. "Microwave characterization of nanostructured material by modified Nicolson-Ross-Weir method." *Ampere Newsletter* 94 (2017): 35-41.
[29] You, Kok Yeow, Man Seng Sim, Hafizah Mutadza, Fahmiruddin Esa, and Yi Lin Chan. "Free-space measurement using explicit, reference-plane and thickness-invariant method for permittivity determination of planar materials." In *2017 Progress in Electromagnetics Research Symposium-Fall (PIERS-FALL)*, pp. 222-228. IEEE, 2017. https://doi.org/10.1109/PIERS-FALL.2017.8293139
[30] Ozturk, Murat, Umur K. Sevim, Oguzhan Akgol, Emin Unal, and Muharrem Karaaslan. "Determination of physical properties of concrete by using microwave nondestructive techniques." *Applied Computational Electromagnetics Society Journal* 33, no. 3 (2018): 265.

[31] Mesquita, Renato C., Elson J. Silva, Fábio Júlio F. Gonçalves, Alfred GM Pinto, and Adriana Brancaccio. "Free-Space Materials Characterization by Reflection and Transmission Measurements using Frequency-by-Frequency and Multi-Frequency Algorithms." *Electronics (2079-9292)* 7, no. 10 (2018). https://doi.org/10.3390/electronics7100260

[32] Wang, J. Y., J. Tao, L. Severac, D. Mesguich, and Ch Laurent. "Microwave characterization of nanostructured material by modified Nicolson-Ross-Weir method." *Ampere Newsletter* 94 (2017): 35-41.

[33] Singh, Harbinder, Balwinder Singh Sohi, and Amit Gupta. "Thickness invariant parameter retrieval techniques for permittivity and permeability measurement." *Journal of Microwave Power and Electromagnetic Energy* 52, no. 3 (2018): 215-239. https://doi.org/10.1080/08327823.2018.1497426

[34] Ozturk, Murat, Umur K. Sevim, Oguzhan Akgol, Emin Unal, and Muharrem Karaaslan. "Determination of physical properties of concrete by using microwave nondestructive techniques." *Applied Computational Electromagnetics Society Journal* 33, no. 3 (2018): 265.

[35] Cuper, Jerzy, Bartłomiej Salski, Paweł Kopyt, Adam Pacewicz, and Adam Raniszewski. "Double-ridged horn antenna operating in 18–40 GHz range." In *2018 22nd International Microwave and Radar Conference (MIKON)*, pp. 304-307. IEEE, 2018. https://doi.org/10.23919/MIKON.2018.8405208

[36] Chudpooti, Nonchanutt, Nattapong Duangrit, Prayoot Akkaraekthalin, Ian D. Robertson, and Nutapong Somjit. "220-320 GHz hemispherical lens antennas using digital light processed photopolymers." *IEEE Access* 7 (2019): 12283-12290. https://doi.org/10.1109/ACCESS.2019.2893230

[37] Tosaka, Toshihide, Katsumi Fujii, Kaori Fukunaga, and Akifumi Kasamatsu. "Development of complex relative permittivity measurement system based on free-space in 220–330-GHz range." *IEEE Transactions on Terahertz science and Technology* 5, no. 1 (2014): 102-109. https://doi.org/10.1109/TTHZ.2014.2362013

[38] Yang, Chuang, Kaixue Ma, and Jian-Guo Ma. "A noniterative and efficient technique to extract complex permittivity of low-loss dielectric materials at terahertz frequencies." *IEEE Antennas and Wireless Propagation Letters* 18, no. 10 (2019): 1971-1975. https://doi.org/10.1109/LAWP.2019.2935170

[39] Kim, Sung, David Novotny, Joshua Gordon, and Jeffrey Guerrieri. "A Thicknessless Method for the Low-Loss Dielectric Characterization from Free-Space Scattering Measurements."

[40] Tosaka, Toshihide, Katsumi Fujii, Kaori Fukunaga, and Akifumi Kasamatsu. "Development of complex relative permittivity measurement system based on free-space in 220–330-GHz range." *IEEE Transactions on Terahertz science and Technology* 5, no. 1 (2014): 102-109. https://doi.org/10.1109/TTHZ.2014.2362013

[41] Alayedi, M., A. Cherifi, A. F. Hamida, C. B. M. Rashidi, and B. S. Bouazza. "Performance improvement of multi access OCDMA system based on a new zero cross correlation code." In *IOP conference series: materials science and engineering*, vol. 767, no. 1, p. 012042. IOP Publishing, 2020. https://doi.org/10.1088/1757-899X/767/1/012042

[42] Ghazi, Alaan, S. A. Aljunid, Syed Zulkarnain Syed Idrus, R. Endut, C. B. M. Rashidi, N. Ali, Aras Al-dawoodi, Ahmed M. Fakhrudeen, Alaa Fareed, and Teena Sharma. "Hybrid WDM and Optical-CDMA over Multi-Mode Fiber Transmission System based on Optical Vortex." In *Journal of Physics: Conference Series*, vol. 1755, no. 1, p. 012001. IOP Publishing, 2021. https://doi.org/10.1088/1742-6596/1755/1/012001